ACS APPLIED MATERIALS & INTERFACES

Forum Article

www.acsami.org

Dynamics of Hyperbranched Polymers under Confinement: A Dielectric Relaxation Study

Krystalenia Androulaki,[†,‡] Kiriaki Chrissopoulou,*[,†] Daniele Prevosto,[§] Massimiliano Labardi,[§] and Spiros H. Anastasiadis*[,†,‡]

[†]Institute of Electronic Structure and Laser, Foundation for Research and Technology−Hellas, 711 10 Heraklion Crete, Greece

[‡]Department of Chemistry, University of Crete, 710 03 Heraklion Crete, Greece

[§]CNR-IPCF, Department of Physics, University of Pisa, Pisa, Italy

ABSTRACT: The effect of severe confinement on the dynamics of three different generations of hyperbranched polyesters of the Boltorn family is investigated by dielectric relaxation spectroscopy (DRS). The polymer chains are intercalated within the galleries of natural montmorillonite (Na^+-MMT), thus forming 1 nm polymer films confined between solid walls. The structure of the nanocomposites is studied with X-ray diffraction and the thermal behavior of the polymers in bulk and under confinement is determined by differential scanning calorimetry. The glass transition temperatures of the polymers show a clear dependence on the generation whereas the transition is completely suppressed when all the polymer chains are intercalated. The dynamic investigation of the bulk polymers reveals two sub-T_g processes, with similar behavior for the three polymers with the segmental relaxation observed above the T_g of each polymer. For the nanocomposites, where all the polymer chains are severely confined, the dynamics show significant differences compared to that of the bulk polymers. The sub-T_g processes are similar for the three generations but significantly faster and with weaker temperature dependence than those in the bulk. The segmental process appears at temperatures below the bulk polymer T_g, it exhibits an Arrhenius temperature dependence and shows differences for the three generations. A slow process that appears at higher temperatures is due to interfacial polarization.

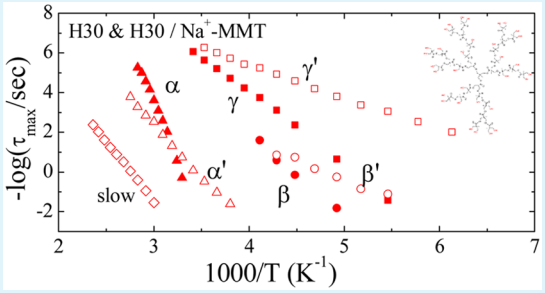

KEYWORDS: *dynamics, dielectric spectroscopy, glass transition, hyperbranched polymers, intercalation, confinement*

I. INTRODUCTION

Dendritic polymers constitute a relatively new class of materials that have attracted the scientific interest because of their unique features like high density, low viscosity, and multiplicity of functional end-groups that make them favorite candidates for numerous applications.[1,2] They can be separated into two broad categories: dendrimers that have symmetric, well-ordered, treelike structure, branches arranged into perfect layers or generations and specified molecular weight; and hyperbranched polymers, HBPs, which have many branch points, as well, but exhibit asymmetric structure and polydispersity. The HBPs show the same unique features of the dendritic macromolecules as low viscosity at high molecular weight, high solubility, miscibility, and reactivity influenced by the end groups, having the additional advantage of a cost-effective synthesis, as compared to dendrimers, because of their one-pot synthetic method and the lack of need for tedious purification procedures. The HBPs can be used in industrial applications;[3,4] as additives in coatings,[5,6] membranes,[7] and batteries;[8] as nanoscale catalysts; additives in conventional epoxy resins;[9] as well as in the pharmaceutical industry and medicine for the encapsulation of substances, targeted delivery of drugs, as therapeutic agents, as in vitro diagnostics for cardiac testing, contrast agents for magnetic resonance imaging (MRI), etc.[10−12]

Up to now, the majority of the experimental studies have addressed issues related to the synthesis and the molecular characterization of hyperbranched polymers,[13−16] and only few with their detailed characterization, their ability to form a hydrogen-bond network, and their structure−property relationship.[17] Moreover, the dynamics of hyperbranched polymers have been investigated experimentally mainly for temperatures lower that the glass transition temperature (T_g),[18−21] utilizing dielectric spectroscopy; quasielastic neutron scattering was also used to investigate the relaxation processes of a HBP showing a significant influence of the hydrogen bonds on the dynamics as compared to linear polymers.[22] Atomistic molecular dynamics simulations have been recently performed, to examine the static and dynamic properties of HBPs in the melt over many length- and time-scales and to investigate the formation and lifetime of both intra- and intermolecular hydrogen bonds.[23,24] Never-

Special Issue: Forum on Polymeric Nanostructures: Recent Advances toward Applications

Received: October 31, 2014
Accepted: January 5, 2015
Published: January 20, 2015

DOI: 10.1021/am507571y
ACS Appl. Mater. Interfaces 2015, 7, 12387−12398

Scheme 1. Three Generations of the Hyperbranched Polyester Polyols Boltorn

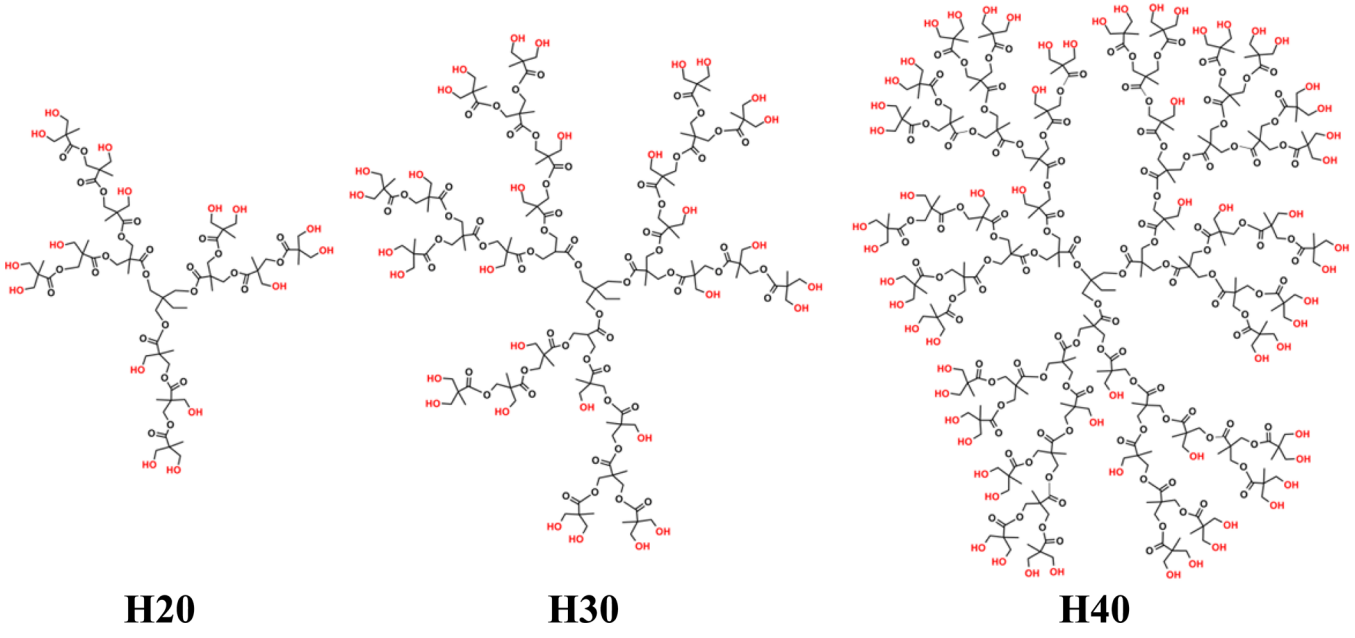

theless, because of their significant advantages and potential applications, there is a need for further investigations aiming at understanding of the microscopic mechanisms responsible for the manifestation of their macroscopic properties.

The investigation of polymer dynamics has been a continuous and intriguing scientific problem through the years, as it influences the structure−property relationship because of the complexity it exhibits over many length- and time-scales.[25,26] Polymer dynamics includes vibrational motions, rotations of side groups, the segmental α-process as well as the overall chain dynamics, thus covering a very broad time regime of more than ten decades from the pico-second (ps) to the second (s) regime.[27] This necessitates the use of different experimental techniques with complementary spatial and temporal capabilities, like, for example, light and neutron scattering[28] and/or dielectric relaxation spectroscopy.[29,30] Among the different techniques, quasielastic neutron scattering and dielectric spectroscopy have been utilized to investigate very local rotation and reorientation of side groups, which are usually observed below the polymer glass transition temperature. These processes hold Arrhenius temperature dependencies, $\tau = \tau_0 \exp[E/RT]$. Above the polymer T_g, these techniques can probe the segmental dynamics or alpha (α) relaxation process exhibited by the macromolecules due to the cooperative motion of chain segments. Characteristic features of this process are the nonexponentiality of the respective relaxation function and the non-Arrhenius temperature dependence of its relaxation time when approaching the T_g, which is empirically described by the Vogel−Fulcher−Tammann equation $\tau \propto \exp[A/(T - T_0)]$.[25,26,28]

More than the investigation of the dynamics of polymers in the bulk, a subject of great interest during recent years is the study of their static and dynamic behavior close to interfaces and/or in very thin films, because significant differences can emerge when the molecules are confined over distances comparable to their sizes.[31−36] The equivalence in the behavior between polymer nanocomposites and thin polymer films has been suggested and quantitatively verified in the case of silica/polystyrene nanocomposites,[37] and studies of the effect of confinement on the glass transition temperature and polymer dynamics have been extended to polymer nanocomposites.[22,38−49]

Among the different nanocomposites, the ones consisting of polymers and layered silicates are considered as a new generation of composite materials because they exhibit unique properties such as enhanced strength and thermal resistance, reduced gas permeability, reduced flammability, etc., which render them candidates for a range of applications.[50−52] These systems can exhibit three different types of structure, the phase separated, the intercalated and the exfoliated one, depending on the interactions between the constituents.[53−55] The intercalated structures, in particular, are ideal systems for studying the properties of macromolecules under strong confinement utilizing, however, macroscopic samples and conventional analytical techniques.

Recent studies on the dynamics of intercalated polymers reveal that the relaxation processes of the bulk polymer are strongly affected by the interaction with the inorganic layers.[38,40,44,46,56−59] A number of investigations showed[38,40,44,56] that the segmental relaxation process (α-relaxation) of the polymer under severe confinement appears at temperatures far below the glass transition temperature of the bulk polymer, the relaxation times are much faster than those in the bulk with an almost Arrhenius temperature dependence. Moreover, the β-relaxation, corresponding to the local motions, is quite similar between the bulk and the confined polymer.[40] In other studies, however, where the polymer-inorganic interactions are more attractive, the α-relaxation observed is much slower than the bulk polymer.[46,57−60]

In the present work, the dynamics of three different generations of a hyperbranched polyester polyol, Boltorn, is investigated in the bulk and, for the first time, under severe confinement when the polymers are intercalated between the layers of layered montmorillonite, Na^+-MMT. The three generations, H20, H30, and H40, further than the different molecular weight, have different number of functional groups both in the periphery and in the interior of the molecules leading to different interactions with the inorganic layers of the

DOI: 10.1021/am507571y
ACS Appl. Mater. Interfaces 2015, 7, 12387−12398

Table 1. Characteristics of Boltorn Hyperbranched Polymers

Boltorn	pseudogeneration	functional groups (−OH)/molecule	theoretical molecular weight (g/mol)	M_w/M_n [a]	T_g [b] (°C)	ΔC_p [b] (cal g^{-1} °C^{-1})
H20	2	16	1750	1.38	14	0.11
H30	3	32	3608	1.40	35	0.11
H40	4	64	7323	1.27	46	0.11

[a]According to the data sheets provided by the supplier (Polymer Factory, Sweden AB). [b]Obtained by DSC measurements.

clay. These systems form a network of intra- and intermolecular hydrogen bonds, which is anticipated to be influenced by the confinement and by the interactions with the surfaces; thus the dynamics is expected to be affected as well. The nanohybrids were prepared by mixing the polymer with natural hydrophilic Na^+-MMT, via a solution-intercalation method. The structure of the nanohybrids was examined by X-ray diffraction and intercalated structures with polymer films of thicknesses of ∼1 nm are obtained for all three generations. Investigation of the thermal properties by differential scanning calorimetry reveals that the glass transition of the polymers shows a dependence on the generation, whereas it is totally suppressed for the confined polymer within the nanohybrids. The polymer dynamics were studied utilizing dielectric relaxation spectroscopy both for the bulk polymers and for the respective intercalated nanocomposites, with ∼50 wt % polymer, where all the polymer is anticipated to more-or-less reside within the filled galleries of the clay. The relaxation processes of the three different generations in the bulk and under confinement, for both the segmental and the sub-T_g processes, are investigated. The segmental relaxation reveals the expected dependence on the generation for the bulk polymers and a significantly different behavior under confinement. The local dynamics of the sub-T_g processes are not affected by the different generations, whereas under confinement, they exhibit lower activation energy and faster relaxation times.

2. EXPERIMENTAL SECTION

Materials. The polymers utilized in this work are the second, third and fourth generation, H20, H30 and H40, of the hyperbranched polyester polyol Boltorn (Scheme 1), supplied by Polymer Factory, Sweden AB. They are amorphous polymers; their branches consist mainly of ester groups and possess a number of hydroxyl end-groups. Therefore, these molecules are highly polar and soluble in polar solvents. Moreover, hydrogen bonds are formed between the hydroxyl groups and ester oxygens, within either the same or different molecules. The molecular characteristics of the polymers are given in Table 1.

The hydrophilic multilayer sodium montmorillonite, Na^+-MMT, Cloisite Na^+, supplied by Southern Clay, was used in this investigation as the inorganic material for the nanocomposites. The natural sodium montmorillonite is a layered silicate clay, which is hydrophilic due to the hydrated cations that exist within its galleries. Because of this hydrophilicity, Na^+-MMT can be mixed with hydrophilic polymers such as Boltorn without the need of any surface modification. The period of the multilayer structure is ∼1 nm (when completely dry) and exhibits a cation exchange capacity, CEC, of 92.6 mmol/100g.

Nanocomposites were prepared via a solution-intercalation method using deionized water as the solvent medium. H20, H30, H40 were mixed with Na^+-MMT, in water, to synthesize a broad range of compositions covering the complete range between pure polymer and pure clay. The required amount of Boltorn polyols was first dissolved in hot water (∼70 °C), and then the respective amount of clay was added under continuous stirring, to ensure that the individual clay layers were well-dispersed.[61] Following mixing, the solvent was evaporated in open air at 70 °C until concentrated slurry was obtained. It was then transferred to a vacuum oven at 70 °C for 48 h. Finally, all samples were triturated and thermally annealed at 200 °C for 24 h, to erase any metastable structure formed during solvent evaporation and to achieve equilibrium.

Fourier transform infrared spectroscopy in the attenuated total reflection mode (FTIR-ATR) was utilized in order to confirm that no degradation occurred during the annealing process under vacuum. Moreover, Thermogravimetric Analysis (TGA) verified the compositions of the synthesized hybrids.

Experimental Techniques. *X-ray Diffraction (XRD).* The structural characterization of the three generations of the hyperbranched polymers and the respective nanocomposites was performed by X-ray diffraction utilizing a RINT-2000 Rigaku Diffractometer. The X-rays are produced by a 12 kW rotating anode generator with a Cu anode and the Cu K_α radiation with wavelength $\lambda = \lambda_{CuK\alpha} = 1.54$ Å is used. Measurements were performed for diffraction angles, 2θ, from 1.5° to 30° with step of 0.02°. The X-ray diffractograms of the layered silicates show the characteristic $(00l)$ peaks due to their periodic structure. These diffraction peaks are related to the spacing of the layers according to Bragg's law, $n\lambda = 2d_{00l} \sin\theta$, where λ is the wavelength of the radiation, d_{00l} the interlayer distance, n the order of diffraction, and 2θ the diffraction angle. Polymer intercalation leads to a shift of the main peak of the pure inorganic clay to lower angles, whereas no peaks are observed in the case of exfoliated structures.

Differential Scanning Calorimetry (DSC). The thermal properties of the three generations of the hyperbranched polymers and the respective nanocomposites were measured with a PerkinElmer Differential Scanning Calorimeter, DSC. The temperature range from −100 to 150 °C was covered with a heating/cooling rate of 10 °C/min. In all cases the glass transition temperature, T_g, was obtained from the second heating cycle, in order to eliminate the thermal history and to remove any remaining humidity. The measurements were performed under constant nitrogen flow to prevent degradation of the samples and controlled cooling was achieved using liquid nitrogen.

Dielectric Relaxation Spectroscopy (DRS). Dielectric spectroscopy measures the dielectric properties of a medium as a function of frequency.[29,30] It is based on the interaction of an external field with the molecular electric dipole moment and the determined quantity is the complex dielectric permittivity

$$\varepsilon^*(\omega) = \varepsilon'(\omega) - i\varepsilon''(\omega) \quad (1)$$

where ε' represents the real part and ε'' the imaginary part or the energy loss part, $\omega = 2\pi\nu$, where ν is the measured frequency. The measured ε^* is given by the one-sided Fourier transform of the time derivative of the dipole−dipole correlation function $C(t)$, which probes local motions unless there is a component of the dipole moment parallel to the chain contour and chain motion is dielectrically active.

The dynamic measurements were performed utilizing a dielectric spectrometer Alpha Analyzer from Novocontrol, in the frequency interval 1×10^{-2} to 1×10^{7} Hz. A film (hundreds of micrometers) of the material under study was placed in a stainless steel parallel plate capacitor. In the case of the pure polymers, the samples were heated at 80 °C and pressed between two plated electrodes with 30 mm diameter. Fused silica fibers with a diameter of 100 μm were used as spacers. The samples were annealed at 140 °C in vacuum for 24 h to remove traces of water. In the case of the nanocomposites, the powder was pressed to form disks 12 mm in diameter and 0.3−0.6 mm in thickness. The pellets were annealed at 140 °C in vacuum for 24 h and adhered between indium foils to improve the electrical contact with the electrodes.

DOI: 10.1021/am507571y
ACS Appl. Mater. Interfaces 2015, 7, 12387−12398

Dielectric spectra of the film were measured isothermally in the range −130−130 °C. The temperature was controlled through a heated flow of nitrogen gas, by a Quatro Cryosystem. During measurements, the samples were kept in a pure nitrogen atmosphere. All samples were kept at the highest starting temperatures for 30 min prior to the measurements and were thermally equilibrated at successively decreasing temperatures before the isothermal data collection.

3. RESULTS AND DISCUSSION

Structural Characterization (XRD). The three generations of Boltorn polyesters in the bulk and in the nanocomposites with varying composition were characterized by X-ray diffraction. Figure 1a shows the XRD measurements of all the

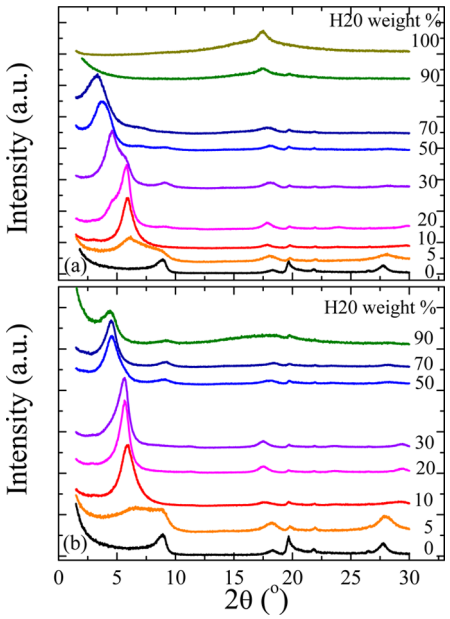

Figure 1. (a) X-ray diffractograms of Na^+-MMT, Boltorn H20, and their nanocomposites after solution mixing and solvent evaporation. (b) X-ray diffractograms of Boltorn H20/Na^+-MMT nanocomposites after thermal annealing at 200 °C under vacuum for 24 h. The curves have been shifted vertically for clarity.

hybrids synthesized utilizing H20, after solution mixing and solvent evaporation, together with the diffractograms of the neat polymer and the pure inorganic material. H20, as well as the other two hyperbranched polymers, are amorphous and they exhibit just a weak amorphous halo shown as a wide peak with full width at half-maximum of ∼4°. On top of this broad peak, there is a sharper one at $2\theta = 17.3°$ that corresponds to a distance of ∼0.5 nm, indicating a chain packing of the polymers that is probably due to an extensive hydrogen bond network.[11,17,24]

The main peak (001) of pure Na^+-MMT is found at $2\theta = 8.9°$, corresponding to an interlayer spacing of $d_{001} = 0.99$ nm for the empty galleries. Addition of H20 (5 wt %) results in a shift of this peak toward lower angles verifying the intercalation of the polymer chains inside the inorganic galleries causing an increase of the interlayer distance. Nevertheless, this peak is very broad, with a shoulder at the interlayer distance of the Na^+-MMT indicating still the presence of empty galleries. Upon further addition of polymer, the shoulder corresponding to the empty galleries disappears and a progressive shift of the main hybrid peak toward lower angles develops. The position of the peak appears at $2\theta = 6.1$, 5.9, 5.8, and 5.7° for 5, 10, 20, and 30 wt %, respectively, and it shifts even more at higher polymer content until, at the highest composition (90 wt % in H20), no peak could be observed, indicating that the specific hybrid has an interlayer distance higher than the highest accessible one. Such an increase in the interlayer distance with polymer content does not indicate equilibrium of the systems since it is well-known that this is defined only by the polymer−inorganic interactions. Moreover, it is noted that for concentrations 20−30 wt % shoulders exist in the diffractograms either on the lower or in the higher diffraction angle regime. A similar behavior had been observed in another hydrophilic nanohybrid synthesized by solution mixing in water, and in that case it was shown that thermal annealing was necessary to achieve the equilibrium structure.[56] Thus, all hybrids were thermally annealed in a vacuum oven at 200 °C for 24 h; their X-ray diffractograms were measured and are shown in Figure 1b. A clear change in the behavior is observed; instead of the gradual increase of the interlayer distance, there are peaks at distinct angles. At low polymer content there is a peak at $2\theta = 5.7° \pm 0.1°$ corresponding to an interlayer spacing of $d_{001} = 1.55 \pm 0.05$ nm whereas above 50 wt % in H20 the peak jumps at $2\theta = 4.5° \pm 0.1°$ corresponding to an interlayer spacing of $d_{001} = 1.95 \pm 0.05$ nm, indicating existence of monolayers and bilayers of polymer chains inside the galleries. In the latter case, the increased coherence of the intercalated structure formed is evident by the existence of a second order diffraction peak at $2\theta = 9.0° \pm 0.1°$, i.e., at an angle at exactly the double value than that of the main diffraction peak. Formation of layers of polymer chains between the surfaces of layered silicates have been observed before for poly(ethylene oxide) both experimentally[41] and computationally[62] as well as for a hyperbranched poly(ester amide).[22] Moreover, at the high diffraction angle range small peaks can be observed that are attributed to the peaks of the pure polymers (at $2\theta = 17.3°$) and of a different crystallographic plane of Na^+-MMT (at $2\theta = 19.7°$).[54] At the lowest polymer concentration, a diffraction peak showing the presence of empty galleries is found as well.

The behavior is very similar for hybrids synthesized with the hyperbranched polymers of higher generations, H30 and H40, as well, i.e., a gradual shift of the diffraction angles with polymer content, which turns into distinct interlayer distances following the thermal annealing that ensures equilibration. Figure 2a shows the comparison of XRD measurements for nanohybrids of H20, H30, and H40 with 50 wt % polymer content after annealing; the respective measurements of the neat polymers are shown in the inset. It is already mentioned that the bulk polymers are amorphous having only a broad peak with a sharper one at $2\theta = 17.3°$ that corresponds to a distance of ∼0.5 nm and indicates a chain packing due to an extensive hydrogen bond network formed mostly between hydroxyl hydrogens and hydroxyl oxygens (OH···OH) and hydroxyl hydrogens and carbonyl oxygens (OH···O═C).[17,24]

Concerning the 50 wt % Boltorn/Na^+-MMT nanocomposites, the intercalated structure is evident in all three cases since the main peak is found shifted with respect to the one of the pure montmorillonite. The position of the peak shows a weak dependence on the generation and is observed at $2\theta = 4.5° \pm 0.1°$ with interlayer spacing $d_{001} = 1.95 \pm 0.05$ nm for H20, at $2\theta = 4.3 \pm 0.1°$ and $d_{001} = 2.05 \pm 0.05$ nm for H30 and $2\theta = 4.1 \pm 0.1°$ and $d_{001} = 2.15 \pm 0.05$ nm for H40. A second-order diffraction peak is observed in all cases because of the increased coherence of the structure. Taking into consideration the

DOI: 10.1021/am507571y
ACS Appl. Mater. Interfaces 2015, 7, 12387−12398

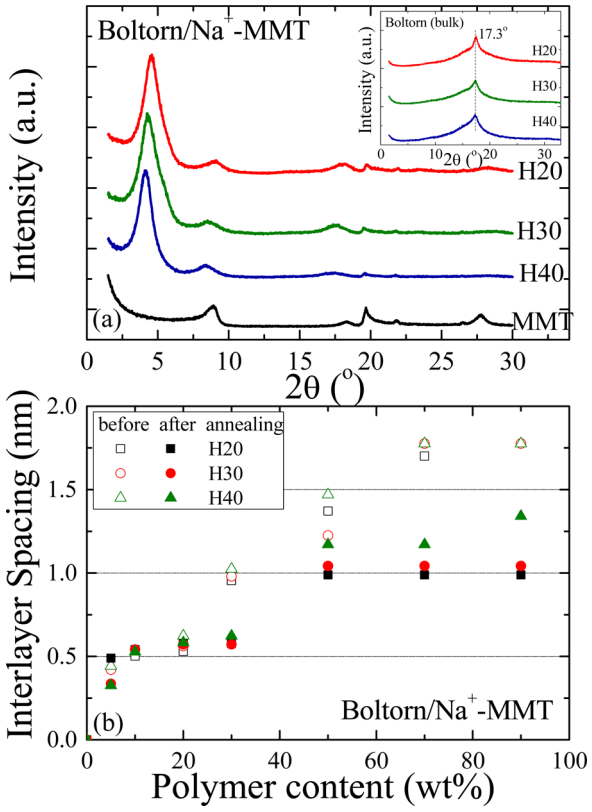

Figure 2. (a) X-ray diffractograms of Na^+-MMT and nanocomposites Boltorn (H20, H30, and H40)/Na^+-MMT with 50 wt % polymer content after annealing at 200 °C. The inset shows the diffractograms of the respective neat polymers. The curves have been shifted vertically for clarity. (b) Polymer content dependence of the interlayer distance of hybrids prepared with solution mixing before (empty symbols) and after (solid symbols) annealing. H20 (□, ■), H30 (○, ●), and H40 (Δ, ▲) nanohybrids.

interlayer spacing of the pure montmorillonite, a thin polymer film of ∼1 nm thickness can be assumed for all hybrids. The interlayer distances of all hybrids for the three generations both before and after annealing are shown in Figure 2b. Before annealing, there is an apparent continuous increase of the interlayer distance with polymer concentration, with the clay retaining its layered structure with simply a higher number of polymer chains inside the galleries (except in the case of 90 wt % of the H20 where either the distance has become too large to be measured or the registry of the structure has been lost). When these hybrids are annealed, interlayer distance d_{001} = 1.5 nm is obtained (2θ = 5.8°) for nanocomposites with low polymer content, very similar for all polymers. For hybrids with polymer content higher than 50 wt % a transition from an interlayer distance of ∼1.5 to ∼2.0 nm is observed. The two distinct distances denote the existence of monolayers and bilayers of polymer chains inside the galleries formed due to the layer by layer intercalation process in water. At 50 wt %, which is the composition of interest for the investigation of the dynamics under confinement, bilayers are formed for all polymers and the macromolecules exist in flatten conformations inside the galleries; atomistic molecular dynamics simulations[11] calculated the radii of gyration, R_g, of these systems as $R_{g,H20} \approx 0.8$ nm and $R_{g,H30} \approx 1.05$ nm (at ambient temperature), i.e., similar to the measured changes in the thicknesses in the intercalated films. What possibly happens in the case of solution mixing and during solvent evaporation is that the polymer chains are trapped in metastable states, albeit with periodic order, probably because of the bulky polymer structure in conjunction with the favorable polymer/surface interactions. When the chains gain enough mobility by thermal annealing, the excess chains deintercalate and the system reaches its equilibrium state. One must, therefore, be very careful in such systems when discussing intercalation or exfoliation of the silicate layers. It is noted that metastable states have been observed in ultrathin polymer films as well.[34,35,63]

Thermal Properties (DSC). The thermal properties of the neat Boltorn polyester polyols of the three generations and of all the nanocomposites were investigated by differential scanning calorimetry (DSC). Figure 3 shows the DSC thermograms of H20, H30, and H40 and of the respective hybrids with 50, 70, and 90 wt % in polymer.

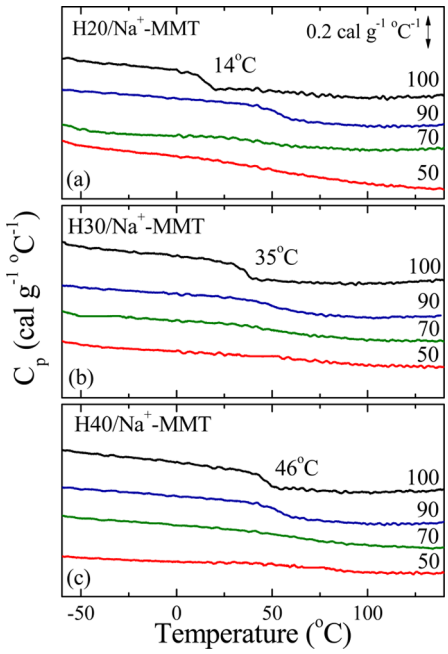

Figure 3. DSC heating curves expressed as specific heat, C_p, for the bulk polymers H20, H30, and H40 and for the nanocomposites Boltorn/Na^+-MMT with 50, 70, and 90 wt % polymer content. (a) H20 and its hybrids, (b) H30 and its hybrids, and (c) H40 and its hybrids. The numbers denote the polymer weight percent. The curves have been shifted vertically for clarity. The vertical scale bar denotes 1 cal g^{-1} °C^{-1}.

DSC confirms the amorphous structure of the macromolecules since only a step in the heat capacity is observed and no melting transition is present. The glass transition temperature of the pure polymers H20, H30 and H40 is obtained at 14 ± 1, 35 ± 1, and 46 ± 1 °C, respectively, i.e., a significant dependence of the T_g on the generation is observed as a consequence of the increased molecular weight and the higher degree of branching. Despite the dependence of the T_g on the generation, the heat capacity step at the transition seems to be constant for the three polymers having the value of ΔC_p = 0.11 ± 0.01 cal.g^{-1}.°C^{-1}.

The DSC thermograms of the three polymers are compared with the respective ones of the intercalated nanocomposites with high polymer content. For the calculation of the heat

DOI: 10.1021/am507571y
ACS Appl. Mater. Interfaces 2015, 7, 12387−12398

capacity, in the case of the hybrids, only the polymer mass is considered, since the contribution of the inorganic material to the C_p is an additive constant that would not influence the step of the glass transition. The respective Boltorn/Na^+-MMT nanocomposites with 50 and 70 wt % polymer content exhibit no identifiable glass transition, as shown in Figure 3 (the same holds for all hybrids with low polymer content). At these polymer concentrations all or most of the polymer chains are confined and the absence of a T_g suggests that the transition is either suppressed because of confinement or too weak or too broad to be detected by DSC. This thermal behavior has been observed before in similar systems of nanohybrids of both linear and hyperbranched polymers.[22,56] For all three kinds of nanocomposites (composed of H20, H30 and H40), only the hybrids with 90 wt % polymer content exhibit a clear glass transition. In all cases, the transition is broader than the respective one of the neat polymers and it is found at higher temperatures. Because at lower concentrations no transition is evident, we attribute the one at 90 wt % to excess polymer chains outside the filled galleries that, nevertheless, interact with the inorganic surfaces causing an increase of the T_g.

Dynamics (DRS). The dynamics of the three hyperbranched Boltorn polyesters were investigated in the bulk and under severe confinement; nanohybrids of 50 wt % H20/Na^+-MMT, 55 wt % H30/Na^+-MMT, and 55 wt % H40/Na^+-MMT were utilized because the structural characterization indicated that at these compositions all polymer chains are intercalated inside filled galleries and there is not excess identifiable polymer outside.

Dynamics were probed by dielectric relaxation spectroscopy in a wide range of frequencies and temperatures, both above and below the glass transition temperature, T_g, of the bulk polymers. Figure 4 shows the imaginary part of the complex permittivity, ε'', for the bulk hyperbranched polymer of second generation, H20, the frequency dependence of which, for the investigated temperature range, reveals multiple relaxation processes. At low temperatures a very broad peak, covering almost 7 orders of magnitude in frequency, is observed, which shifts at higher frequencies as temperature increases. This sub-T_g relaxation peak can reflect to the motion of hydroxyl groups and/or the orientation fluctuations of the ester groups, the so-called γ- and β-process, respectively, according to the literature.[18−21] All three generations of the hyperbranched polyester polyols investigated, exhibit this broad peak at temperatures below 10 °C showing very similar characteristics. At temperatures around the calorimetric glass transition, another peak appears which is related to glassy dynamics (α-process) as identified by the quantitative analysis which is presented below. At even higher temperatures (333−363 K, depending on the generation) the observation of any relaxation processes is partially obscured by the conductivity contribution in all the three polymers. The dynamics of similar hyperbranched polymers have been studied in the past by dielectric spectroscopy. In the past, two distinct sub-T_g processes associated with the hydroxyl motion and the ester reorientation respectively, were observed with similar activation energies, E, in the case of hydroxyl-terminated polymers. On the other hand in hyperbranched polyesters with terminal acetate, benzoate or aliphatic groups only one peak, attributed to the ester group, was observed but with much larger E.[18,19] In another study, where the dynamics of the H20, H30, H40, and H50 hyperbranched polymers was investigated, only one peak was observed, at low temperatures, identified as the γ-process because all other peaks were covered by the effect of conductivity.[20] Finally, the most recent work that investigated the dynamics of the same four generations of hyperbranched polymers resolves the γ- and the β-processes below the glass transition temperature and no other relaxation process above T_g.[21] In general, to the best of our knowledge, there is no investigation up to now that clearly identifies the segmental α-relaxation in the second, third, and fourth generations of hydroxyl terminated hyperbranched polymers.

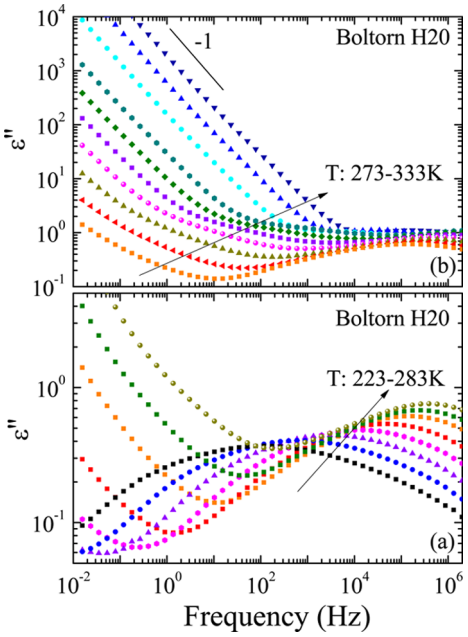

Figure 4. Frequency dependence of the imaginary part of the dielectric permittivity, ε'', for the H20 neat polymer at a temperature range of (a) 223−283 and (b) 273−333 K.

Besides the pure polymers, DRS measurements were performed for the three nanocomposites comprising 50 wt % Boltorn and 50 wt % Na^+-MMT. Figure 5 shows the imaginary part of the complex dielectric permittivity for H20/Na^+-MMT in a very broad temperature range; it is noted that the accessible temperatures for the hybrid materials cover a much broader range than for the respective polymers both for the low- and the high-temperature regime. Clear differences are observed in the spectra of the hybrid compared with the ones of H20 both below and above the T_g of the bulk polymer. At low temperatures, the spectra seem to have multiple relaxation processes like in the case of the pure polymer; nevertheless, all curves have a very different shape with lower dielectric strength and significantly faster relaxation times than the bulk (when compared at the same temperature). For higher temperatures, but still below the glass transition temperature of neat H20 (note that for the specific hybrid, no calorimetric T_g has been observed by DSC), the presence of an additional process becomes evident. In studies of the dynamics of linear polymers confined within the galleries of layered silicates, a process with an Arrhenius temperature dependence, which was observed below the polymer glass transition temperature, was identified as the segmental relaxation, which was significantly modified due to confinement.[38,41] The same conclusion was drawn for other glass formers in nanopores.[64−66]

For even higher temperatures (above 300 K), an additional process appears, which is not present in the neat polymers

DOI: 10.1021/am507571y
ACS Appl. Mater. Interfaces 2015, 7, 12387−12398

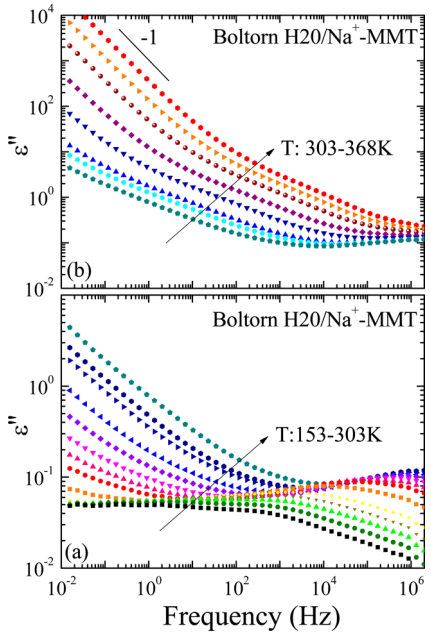

Figure 5. Frequency dependence of the imaginary part of the dielectric permittivity, ε'', for the H20/Na^+-MMT with 50 wt % polymer content at a temperature range of (a) 153−303 and (b) 303−368 K.

either because it was obscured by conductivity or because it indeed exists only in hybrids due to either the confinement or to the presence of the surfaces. The behavior is qualitatively very similar between the three nanohybrids with ∼50 wt % of H20, H30, and H40 and all relaxation processes are evident in all nanocomposites. To differentiate the processes, we will name those in nanocomposites with the same greek letter followed by a prime apex (α', β', γ')

Quantitative comparison on the relaxation processes and their characteristic times was performed both between the three different generations of the polymers and between the polymers in the bulk and under confinement in the nanohybrids. The $\varepsilon^*(\omega)$ data were analyzed utilizing the empirical Havriliak−Negami (HN) functions[30]

$$\varepsilon^*(\omega) = \varepsilon_\infty + \Delta\varepsilon/[1 + (i\omega\tau_{HN})^\alpha]^\beta \quad (2)$$

where τ_{HN} is the characteristic relaxation time, $\Delta\varepsilon = \varepsilon_0' - \varepsilon_\infty'$ is the relaxation strength of the process, and α, β ($0 < \alpha$, $\alpha\beta \leq 1$) describe the symmetric and asymmetric broadening of the distribution of relaxation times. An additional ionic conductivity contribution at low-frequencies and high temperatures is accounted for by an ω^{-1} dependence. Figure 6 demonstrates the representative analysis of the spectra for three temperatures, below, slightly above and much above the T_g of the second generation hyperbranched polymer, Boltorn H20, in the bulk and for the respective 50 wt % nanocomposite. From the analysis, it appears that in all cases, multiple relaxation processes are necessary to obtain a good fit to the data. From the spectra at low temperatures, the shape and relaxation strength parameters are determined for the γ- and β- processes of both the bulk polymer and the nanocomposite. In the bulk, for the γ-process the β parameter is fixed to 0.8 for H20, 0.9 for H30, and 1.0 for H40, whereas the α (0.2−0.3) and $\Delta\varepsilon$ (2.8−6.7) parameters increase with increasing temperature. At higher temperatures, above T_g, for the bulk polymers the α-process emerges, as shown in Figure 6c, e (dash-dotted line); for this process and for all three polymers, the β parameter is fixed at 1.0, whereas α is determined around 0.36−0.45 and $\Delta\varepsilon$ is constantly decreasing from 9.3 to 3.7.

For the nanocomposites of all three generation polymers, the β parameter of the γ' process (Figure 6b−dashed line) is fixed to 1.0; temperature dependent α parameter (0.23−0.31) and $\Delta\varepsilon$ (0.2−0.87) values were utilized with the dependencies derived from the low temperature spectra. At higher temperatures, below the bulk polymer T_g, an intermediate process appears (Figure 6d−dash-dotted line) and, at even higher temperatures, a slow process (dash-dot-dot line) becomes evident. For both the intermediate and the slow process the β parameter is fixed at 1.0. The α parameter of the intermediate process for all three nanocomposites is around 0.26−0.5 and $\Delta\varepsilon$ decreases from 0.7 to 0.12; for the slow process, α is around 0.45−0.53, whereas $\Delta\varepsilon$ increases from 9 to 32. At low frequencies and high temperatures, the addition of a contribution due to ionic conductivity is necessary as a line with a slope of ∼0.92−0.98; nevertheless, it is noted that the conductivity is significantly lower for the three nanocomposites than for the respective neat polymers. It is emphasized that in all cases the β process can be resolved only in a limited range of temperatures and thus the obtained parameters are not mentioned here.

Figure 7 shows the results of the above analysis concerning the relaxation times in an Arrhenius representation. For the three bulk hyperbranched polymers (Figure 7a), the relaxation times of the γ- and the β-processes coincide and follow an Arrhenius temperature dependence, $\tau = \tau_0 \exp[E/RT]$. The activation energies of the γ-process are $E_{\gamma,H20}$ = 65.0 ± 1.5 kJ/mol, $E_{\gamma,H30}$ = 69.5 ± 1.0 kJ/mol and $E_{\gamma,H40}$ = 66.5 ± 1.5 kJ/mol and τ_0 = O(1×10^{-18} s), respectively (R is the gas constant). This process is due to local fluctuations and rotations of the hydroxyl groups. It is noted that the values that we report for the activation energies of the γ-process of the neat polymers are lower than the ones reported in the literature[18,19,21] but still high in comparison to local processes of linear polymers.[41] As far as the intermediate β-process is concerned, there are few temperatures from which we can derive a relaxation time since, as temperature increases, it is in close proximity to the other two processes. The temperature dependence of its relaxation times seems very similar to the one of the γ-relaxation. The activation energies derived for the three polymers are $E_{\beta,H20}$ = 70 ± 3 kJ/mol, $E_{\beta,H30}$ = 81 ± 9 kJ/mol, and $E_{\beta,H40}$ = 86 ± 2 kJ/mol, respectively. For this process, an apparent dependence of the activation energy on the generation is observed probably indicating that the reorientation of the carbonyl groups becomes more difficult as the molecules become more dense. Around the T_g of each polymer, as determined by DSC, the segmental process appears. For this process a different behavior is observed between the three polymers, as expected, due to the differences of the calorimetric glass transition of the three generations. Moreover, the temperature dependence of this process appears to follow the Vogel−Fulcher−Tammann (VFT) equation $\tau = \tau_0 \exp[B/(T - T_0)]$. The parameters obtained from the fit with VFT expression bare significant error, especially in cases that the range of the experimental data is limited. To minimize the error in the analysis, the value of $\tau_0 = 1 \times 10^{-13}$ is kept fixed for all samples. The resulted parameters are B = 1939 ± 29 K and T_0 = 225.6 ± 1.0 K for H20, B = 2113 ± 24 K, and T_0 = 233.5 ± 1.0 K for H30 and B = 2227 ± 29 K and T_0 = 237.3 ± 1.0 K for H40. The Vogel temperature T_0 increases with generation and shows a similar dependence with that of the calorimetric glass transition

DOI: 10.1021/am507571y
ACS Appl. Mater. Interfaces 2015, 7, 12387−12398

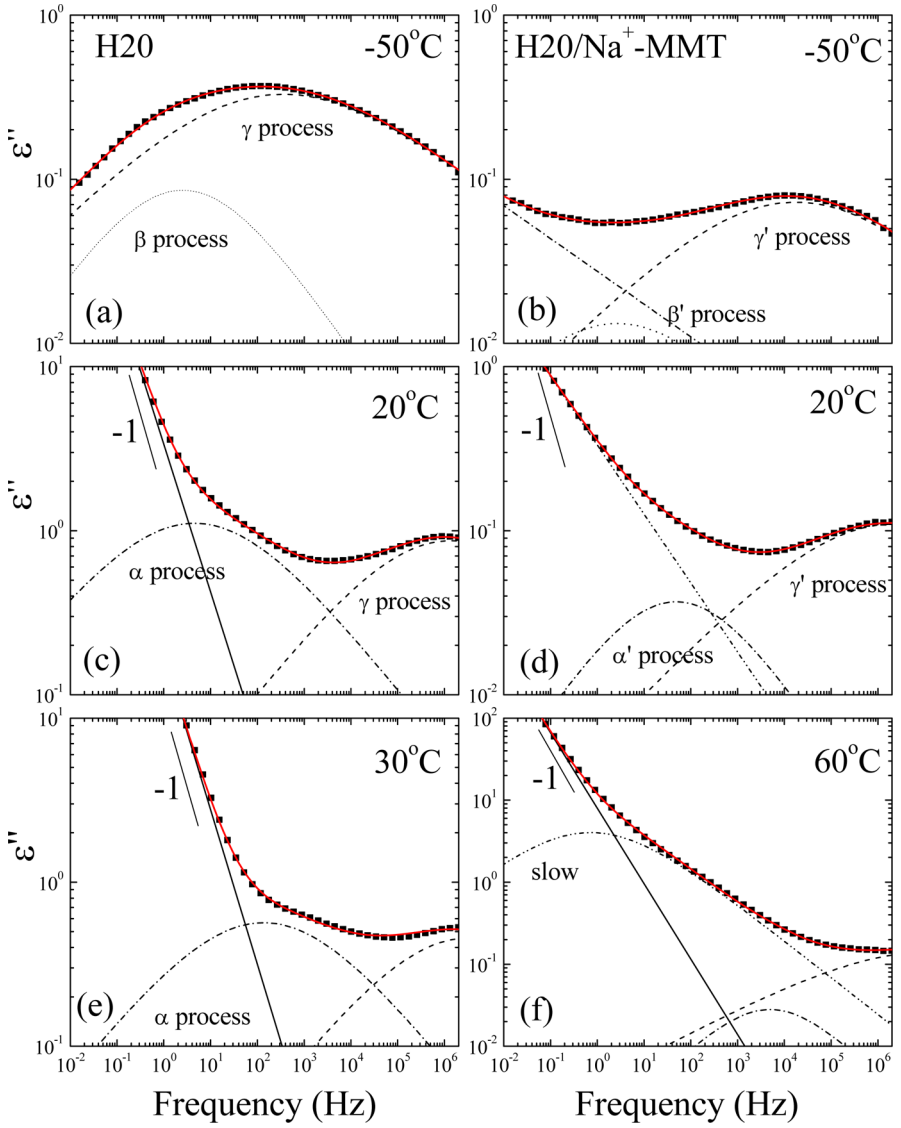

Figure 6. Imaginary part of the dielectric permittivity, ε'', (a, c, e) for the H20 and (b, d, f) for the H20/Na^+-MMT with 50 wt % polymer weight at (a, b) 223, (c, d) 293, (e) 303, and (f) 333 K. The processes needed for the deconvolution of the spectra are shown with dashed (γ and γ'), dotted (β and β'), dash-dotted (α and α'), and dash-dot-dot (slow) lines, whereas the solid lines are the convolution of the processes (together with the conductivity at high temperatures).

temperature, as anticipated. Moreover, the fragility parameter is D = 8.6, 9.0, and 9.4 for H20, H30, and H40, respectively denoting that the increase in the generation results in slightly stronger glasses.

On the other hand, the nanocomposites exhibit a different scenario for both the sub-T_g and the segmental dynamics. Figure 7b shows the relaxation times of the different processes present for all nanohybrids. It is noted that, according to recent studies on linear polymers, such as poly(ethylene oxide), confined within the galleries of layered silicate, the sub-T_g (β'-) process was not affected by the confinement, while the segmental relaxation (α'- process) was observed below the bulk polymer T_g, with an almost Arrhenius temperature dependence.[41] Moreover, quasielastic neutron scattering measurements on the hyperbranched poly(ester−amide) Hybrane showed that the very local sub-T_g dynamics exhibit similar behavior in the bulk and under confinement;[22] this process was attributed to a methyl and/or hydroxyl group rotation which could be coupled and also affected by both intra- and intermolecular hydrogen bonds that are formed in these hyperbranched systems.

Two sub-T_g processes exist in the case of the three nanocomposites as well; nevertheless, their relaxation times are much faster than the respective ones of the neat polymers and with much weaker Arrhenius temperature dependence. On the other hand, both processes have very similar relaxation times when the three confined polymers are compared. For the fastest process, called γ', the activation energies that result from the temperature dependence of the relaxation times have values $E_{\gamma',H20}$ = 32.5 ± 2.5 kJ/mol, $E_{\gamma',H30}$ = 31 ± 2 kJ/mol, and $E_{\gamma',H40}$ = 23 ± 1 kJ/mol. This process is identified as the motion of the polar hydroxyl groups of the confined chains. It is noted that these values are very similar to the activation energy obtained for the sub-T_g process for a linear poly(ethylene oxide), the dynamics of which was measured with DRS.[41] Because a difference between the case of the linear PEO and the Boltorn hyperbranched polymers of the current work is the ability of the latter to form hydrogen bonds, we attribute the high

DOI: 10.1021/am507571y
ACS Appl. Mater. Interfaces 2015, 7, 12387−12398

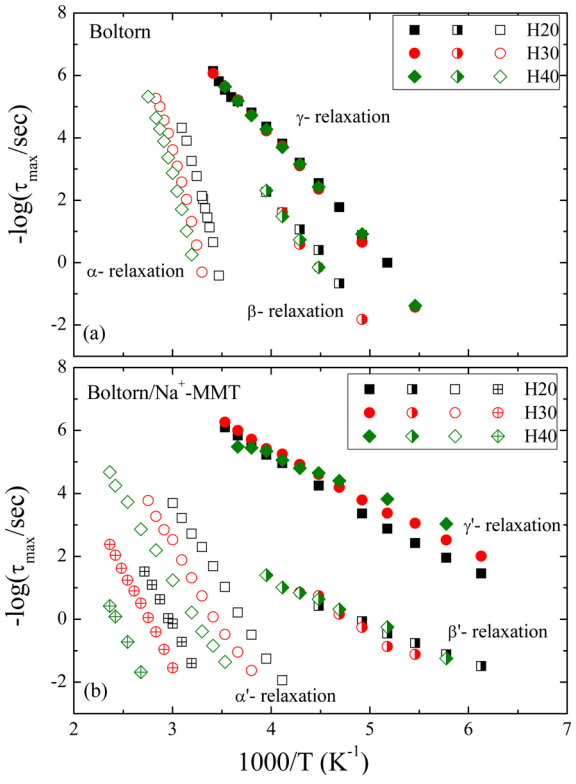

Figure 7. Arrhenius relaxation map for the (a) H20, H30, H40 neat hyperbranched polymers and (b) for Boltorn/Na^+-MMT nanocomposites with 50 wt % polymer. The processes are indicated as follows: the γ- and γ'-processes (filled symbols), the β- and β'-processes (half-filled symbols), the α- and α'-processes (open symbols), and the slow-processes (open crossed symbols). H20 (squares), H30 (circles), and H40 (diamonds).

activation energies of the Boltorns to the hindrance in the motion imposed by the network formed. Under confinement, the flattened conformation that the polymers assume because of the spatial restrictions is not appropriate for the hydrogen bonds to form, causing the activation energy for the respective motion to be lower than the one of the bulk, and to approach the value obtained for a non-hydrogen bonded system. The second sub-T_g process, called β', shows similar temperature dependence to the γ' process. The activation energies for this process are $E_{\beta',H20}$ = 23.5 ± 1.0 kJ/mol, $E_{\beta',H30}$ = 32.5 ± 2.5 kJ/mol, and $E_{\beta',H40}$ = 26 ± 1 kJ/mol. The easier carbonyl reorientation is attributed to the less restricted motion due to the fewer hydrogen bonds in this case as well. At higher temperatures, even more significant deviations in the behavior between the pure polymer and the nanohybrids appear. First, there is an intermediate process that emerges at temperatures much below the bulk polymer T_g, with an Arrhenius temperature dependence. This behavior resembles the α'-process, observed in previous studies on PMPS[38] and PEO[41] under confinement. In the case of the Boltorns, the α'-process is much faster than the one of the neat polymers for lower temperatures or in the proximity of the glass transition temperature but, at higher temperatures, it appears to cross the α-process of the bulk polymer becoming much slower. The dielectric strength of the α' process decreases with increasing temperature that is a property typical of the segmental relaxation. Also the activation energy of the process suggests that it is not related to the motion of a single subunit. In fact, their values are very high: $E_{\alpha',H20}$ = 99.4 kJ/mol, $E_{\alpha',H30}$ = 100.7 kJ/mol, and $E_{\alpha',H40}$ = 99.2 kJ/mol, whereas they are very similar for the three confined polymers. Nevertheless, it appears in the frequency window at higher temperatures with increasing the generation (−30, −10, and 10 °C). Additionally, the difference between the bulk T_g and the temperature at which the α'-process appears seems to be rather similar for the three generations (H20, 44 °C; H30, 45 °C; and H40, 36 °C). It is stressed once more that DSC did not show any thermal transitions for the hybrids with 50 wt % polymer content, whereas, for high compositions, where a transition was indeed observed its temperature was higher that the respective of the pure polymers. Nevertheless, the observed dynamic behavior indicates enhanced mobility at even lower temperatures (below the T_g). A discrepancy in the glass transition temperatures of thin films measured by dilatometry and derived by DRS was reported before for films of hyperbranched polymers with various thicknesses;[67] nevertheless, even the thinnest film of that work was much thicker than the ∼1 nm confining length within the galleries of the layered silicates. Even for those thicker films, an increasing T_g with film thickness was measured by dilatometry whereas a strongly decreasing one was obtained by the dynamic measurements. Moreover, in recent years, the possible decoupling between the thickness dependence of the thermodynamic glass transition temperature, as measured by dilatometry or DSC, and dynamic glass transition temperature, as measured by dielectric spectroscopy, in pure polymer ultrathin films, is debated.[68,69] Another possible interpretation is as follows. Confinement effects are schematically divided in interfacial effects, that can speed up or slow down the dynamics according to the kind of interactions between the polymer and the confining medium, and pure geometrical effects, that produce a speed up of dynamics due to reduction of cooperatively rearranging regions. Accordingly, one can suppose that at high polymer content, when there is excess polymer that is not confined within the ∼1 nm galleries, interfacial effects produce the increase of T_g. However, when the polymer content in hybrids decreases and polymer chains are restricted in ∼1 nm layers, the cooperativity is largely reduced, and this effect prevails on the interfacial one.[70] This effect was already observed, although less clearly, in a previous work on nanocomposite materials.[58]

Finally, at even higher temperatures, a slow process appears, for all confined systems, probably due to interfacial polarization because of the large number of interfaces constituting the nanocomposites and the ions trapped in their proximity. This process shows an Arrhenius temperature dependence and a significant effect on the generation as well.

4. CONCLUSIONS

The dynamic behavior of three different generations of the hyperbranched polyesters Boltorn under severe confinement was investigated and was compared with the respective ones of the neat polymers. The confinement is imposed by the intercalation of the chains within the galleries of a hydrophilic sodium montmorillonite, Na^+-MMT, and the effect of the varying interactions with the surfaces caused by the increased number of functional groups was studied. The intercalated structure was verified by XRD, evidencing that after thermal annealing the chains in all three cases form structures with mono- and bilayers of polymer chains inside the galleries. The thermal behavior was investigated with DSC. A glass transition that showed a significant dependence on the generation was

DOI: 10.1021/am507571y
ACS Appl. Mater. Interfaces 2015, 7, 12387−12398

evidenced for the neat polymers, whereas it was suppressed for most of the nanohybrids when the chains were intercalated. Only for nanocomposites with very high polymer content, the glass transition was probed with the temperature being higher than the respective one of the neat polymers. The dynamics of the three polymers and their nanohybrids with ∼50 wt % polymer were investigated with DRS and showed multiple relaxation processes across the whole temperature range.

Two sub-T_g processes identified as γ and β, i.e., as the local hydroxyl and carbonyl motions, are found with Arrhenius temperature dependencies and large activation energies due to the restrictions imposed by the hydrogen-bond network. The same processes are found under confinement but with significant alterations in their behavior. Both are faster than the ones of the neat polymers and with weaker temperature dependencies indicating that hydrogen bonds cannot be formed under this confinement and, thus, the motion becomes less restricted. The segmental relaxation reveals the expected dependence on the T_g and, thus, on the generation for the bulk polymers and a significantly different behavior under confinement; in the latter case, it emerges below the respective bulk polymer T_g with Arrhenius temperature dependence and a significant dependence on the generation. The effect of confinement on the segmental dynamics is related to the interactions with the inorganic component.

Hyperbranched polymers can be utilized in numerous applications that cover almost all range from commodity materials for everyday use to more advanced materials like for example coatings, membranes and batteries, as well as for applications in the pharmaceutical industry and medicine. On the other hand, addition of appropriate nanomaterials into polymers is utilized to improve the polymer properties by taking advantage of the presence of many interfaces with different interactions. In all these cases, knowledge of the structure and the dynamics in the bulk and close to surfaces is important since it is the dynamics that greatly affects the macroscopic properties. The Boltorn family utilized in the present work are commercial materials, which have already been used in applications like hosts for the multifunctional bioactive agents[11] or proton conducting organic−inorganic hybrid membranes,[7] i.e., for applications in the bulk as well as close to inorganics, and thus, knowledge of their structure and dynamics can widen their range of potential applications.

AUTHOR INFORMATION

Corresponding Authors

*E-mail: spiros@iesl.forth.gr.
*E-mail: kiki@iesl.forth.gr.

Notes

The authors declare no competing financial interest.

ACKNOWLEDGMENTS

This research has been cofinanced by the European Union (ESF) and Greek national funds through the Operational Program "Education and Lifelong Learning" of the NSRF - Research Funding Program: THALES - Investing in knowledge society through the European Social Fund (MIS 377278) and the COST Action MP0902-COINAPO (STSM-MP0902-14971).

DEDICATION

Dedicated to Professor Manfred Stamm on the occasion of his 65th birthday

REFERENCES

(1) Tomalia, D. A. The Dendritic State. *Mater. Today* **2005**, *8*, 35−46.
(2) Yan, D.; Gao, C.; Frey, H. *Hyperbranched Polymers: Synthesis, Properties and Applications*; Wiley Series on Polymer Engineering and Technology; Wiley: New York, 2011.
(3) Gillies, E. R.; Frechet, J. M. J. Dendrimers and Dendritic Polymers in Drug Delivery. *Drug Discovery Today* **2005**, *10*, 35−43.
(4) Voit, B. I.; Lederer, A. Hyperbranched and Highly Branched Polymer Architectures − Synthetic Strategies and Major Characterization Aspects. *Chem. Rev.* **2009**, *109*, 5924−5973.
(5) Mulkern, T. J.; Tan, N. C. B. Processing and Characterization of Reactive Polystyrene/Hyperbranched Polyester Blends. *Polymer* **2000**, *41*, 3193−3203.
(6) Ratna, D.; Varley, R.; Simon, G. P. Processing and Chemorheology of Epoxy Resins and their Blends with Dendritic Hyperbranched Polymers. *J. Appl. Polym. Sci.* **2004**, *92*, 1604−1610.
(7) Zou, J.; Zhao, Y.; Shi, W. Preparation and Properties of Proton Conducting Organic-Inorganic Hybrid Membranes based on Hyperbranched Aliphatic Polyester and Phosphoric Acid. *J. Membr. Sci.* **2004**, *245*, 35−40.
(8) Wang, X.; Liu, H.; Jin, Y.; Chen, C. Polymer-functionalized Multiwalled Carbon Nanotubes as Lithium Intercalation Hosts. *J. Phys. Chem. B* **2006**, *110*, 10236−10240.
(9) Pettersson, B. Hyperbranched Polymers: Unique Design Tools for Multi-property Control in Resins and Coatings. *Pigm. Resin Technol.* **1996**, *25*, 4−14.
(10) Chen, S.; Zhang, X. Z.; Cheng, S. X.; Zhuo, R. X.; Gu, Z. W. Functionalized Amphiphilic Hyperbranched Polymers for Targeted Drug Delivery. *Biomacromolecules* **2008**, *9*, 2578−2585.
(11) Tanis, I.; Karatasos, K.; Assimopoulou, A. N.; Papageorgiou, V. P. Modelling of Hyperbranched Polyesters as Hosts for the Multifunctional Bioactive Agent Shikonin. *Phys. Chem. Chem. Phys.* **2011**, *13*, 11808−11817.
(12) Zeng, X.; Zhang, Y.; Wu, Z.; Lundberg, P.; Malkoch, M.; Nystrom, A. M. Hyperbranched Copolymer Micelles as Delivery Vehicles of Doxorubicin in Breast Cancer Cells. *J. Polym. Sci., Part A: Polym. Chem.* **2012**, *50*, 280−288.
(13) Gelade, E. T. F.; Goderis, B.; de Koster, C. G.; Meijerink, N.; van Benthem, R.; Fokkens, R.; Nibbering, N. M. M.; Mortensen, K. Molecular Structure Characterization of Hyperbranched Polyesteramides. *Macromolecules* **2001**, *34*, 3552−3558.
(14) Froehling, P. Development of DSM's Hybrane hyperbranched polyesteramides. *J. Polym. Sci., Part A: Polym. Chem.* **2004**, *42*, 3110−3115.
(15) Zagar, E.; Zigon, M.; Podzimek, S. Characterization of Commercial Hyperbranched Aliphatic Polyesters. *Polymer* **2006**, *47*, 166−175.
(16) Dritsas, G. S.; Karatasos, K.; Panayiotou, C. Investigation of Thermodynamic Properties of Hyperbranched Aliphatic Polyesters by Inverse Gas Chromatography. *J. Chromatogr. A* **2009**, *1216*, 8979−8985.
(17) Zagar, E.; Huskic, M.; Zigon, M. Structure-to-Properties Relation of Aliphatic Hyperbranched Polyesters. *Macrom. Chem. Phys.* **2007**, *208*, 1379−1387.
(18) Malmstrom, E.; Liu, F.; Boyd, R. H.; Hult, A.; Gedde, U. W. Relaxation Processes in Hyperbranched Polyesters. *Polym. Bull.* **1994**, *32*, 679−685.
(19) Malmstrom, E.; Hult, A.; Gedde, U. W.; Liu, F.; Boyd, R. H. Relaxation Processes in Hyperbranched Polyesters: Effect of Terminal Groups. *Polymer* **1997**, *38*, 4873−4879.
(20) Zhu, P. W.; Zheng, S.; Simon, G. Dielectric Relaxation in a Hyperbranched Polyester with Terminal Hydroxyl Groups: Effects of Generation Number. *Macromol. Chem. Phys.* **2001**, *202*, 3008−3017.

DOI: 10.1021/am507571y
ACS Appl. Mater. Interfaces 2015, 7, 12387−12398

(21) Turky, G.; Shaaban, S. S.; Schoenhals, A. Broadband Dielectric Spectroscopy on the Molecular Dynamics in Different Generations of Hyperbranched Polyester. *J. Appl. Polym. Sci.* **2009**, *113*, 2477−2484.
(22) Fotiadou, S.; Karageorgaki, C.; Chrissopoulou, K.; Karatasos, K.; Tanis, I.; Tragoudaras, D.; Frick, B.; Anastasiadis, S. H. Structure and Dynamics of Hyperbranched Polymer/Layered Silicate Nanocomposites. *Macromolecules* **2013**, *46*, 2842−2855.
(23) Tanis, I.; Tragoudaras, D.; Karatasos, K.; Anastasiadis, S. H. Molecular Dynamics Simulations of a Hyperbranched Poly(ester amide): Statics, Dynamics and Hydrogen Bonding. *J. Phys. Chem. B* **2009**, *113*, 5356−5368.
(24) Tanis, I.; Karatasos, K. Local Dynamics and Hydrogen Bonding in Hyperbranched Aliphatic Polyesters. *Macromolecules* **2009**, *42*, 9581−9591.
(25) Sakai, V. G.; Arbe, A. Quasielastic Neutron Scattering in Soft Matter. *Curr. Opin. Colloid Interface Sci.* **2009**, *14*, 381−390.
(26) Chen, K.; Saltzman, E. J.; Schweizer, K. S. Segmental Dynamics in Polymers: from Cold Melts to Ageing and Stressed Glasses. *J. Phys.: Condens. Matter* **2009**, *21*, 503101.
(27) Frick, B.; Richter, D. The Microscopic Basis of the Glass-Transition in Polymers from Neutron-scattering Studies. *Science* **1995**, *267*, 1939−1945.
(28) Colmenero, J.; Arbe, A. Recent Progress on Polymer Dynamics by Neutron Scattering: From Simple Polymers to Complex Materials. *J. Polym. Sci., Part B: Polym. Phys.* **2013**, *51*, 87−113.
(29) Runt, J. P.; Fitzgerald, J. J. *Dielectric Spectroscopy of Polymeric Materials: Fundamentals and Applications*; American Chemical Society: Washington, D.C., 1997.
(30) Schonhals, A.; Kremer, F. *Broadband Dielectric Spectroscopy*; Springer: Berlin, 2003.
(31) Keddie, J. L.; Jones, R. A. L.; Cory, R. A. Size-Dependent Depression of the Glass transition Temperature in Polymer Films. *Europhys. Lett.* **1994**, *27*, 59−64.
(32) O'Connel, P. A.; Mc Kenna, G. B. Rheological Measurements of the Thermoviscoelastic Response of Ultrathin Polymer Films. *Science* **2005**, *307*, 1760−1763.
(33) Zorn, R.; L. van Eijck, Koza, M. M.; Frick, B.; , Eds.; Special Issue on "Progress in Dynamics in Confinement *Eur. Phys. J.: Spec. Top.* **2010**, *189*, 1−302. McKenna, G. B. *Eur. Phys. J.: Spec. Top.* **2010**, *189*, 285−302.
(34) Napolitano, S.; Wübbenhorst, M. The Lifetime of the Deviations from Bulk Behaviour in Polymers Confined at the Nanoscale. *Nature Commun.* **2011**, *2*, 260.
(35) Nguyen, H. K.; Labardi, M.; Capaccioli, S.; Lucchesi, M.; Rolla, P.; Prevosto, D. Interfacial and Annealing Effects on Primary α-Relaxation of Ultrathin Polymer Films Investigated at Nanoscale. *Macromolecules* **2012**, *45*, 2138−2144.
(36) Ngai, K. L.; Prevosto, D.; Grassia, L. Viscoelasticity of Nanobubble-Inflated Ultrathin Polymer Films: Justification by the Coupling Model. *J, Polym. Sci., Part B: Polym. Phys.* **2013**, *51*, 214−224.
(37) Bansal, A.; Yang, H.; Li, C.; Cho, K.; Benicewicz, B. C.; Kumar, S. K.; Schadler, L. S. Quantitative Equivalence between Polymer Nanocomposites and Thin Polymer Films. *Nat. Mater.* **2005**, *4*, 693−698.
(38) Anastasiadis, S. H.; Karatasos, K.; Vlachos, G.; Manias, E.; Giannelis, E. P. Nanoscopic-confinement Effects on Local Dynamics. *Phys. Rev. Lett.* **2000**, *84*, 915−918.
(39) Ash, B. J.; Siegel, R. W.; Schadler, L. S. Glass-transition Temperature Behavior of Alumina/PMMA Nanocomposites. *J. Polym. Sci., Part B: Polym. Phys.* **2004**, *42*, 4371−4383.
(40) Frick, B.; Alba-Simionesco, C.; Dosseh, G.; Le Quellec, C.; Moreno, A. J.; Colmenero, J.; Schonhals, A.; Zorn, R.; Chrissopoulou, K.; Anastasiadis, S. H.; Dalnoki-Veress, K. Inelastic Neutron Scattering for investigating the dynamics of confined glass-forming liquids. *J. Non-Cryst. Sol.* **2005**, *351*, 2657−2667.
(41) Elmahdy, M. M.; Chrissopoulou, K.; Afratis, A.; Floudas, G.; Anastasiadis, S. H. Effect of Confinement on Polymer Segmental Motion and Ion Mobility in PEO/Layered Silicate Nanocomposites. *Macromolecules* **2006**, *39*, 5170−5173.
(42) Chrissopoulou, K.; Afratis, A.; Anastasiadis, S. H.; Elmahdy, M. M.; Floudas, G. Structure and Dynamics in PEO Nanocomposites. *Europ. Phys. J.-Sp. Top.* **2007**, *141*, 267−271.
(43) Rittigstein, P.; Priestley, R. D.; Broadbelt, L. J.; Torkelson, J. M. Model Polymer Nanocomposites Provide an Understanding of Confinement Effects in Real Nanocomposites. *Nat. Mater.* **2007**, *6*, 278−282.
(44) Chrissopoulou, K.; Anastasiadis, S. H.; Giannelis, E. P.; Frick, B. Quasielastic Neutron Scattering of Poly(methyl phenyl siloxane) in Bulk and Under Severe Confinement. *J. Chem. Phys.* **2007**, *127*, 144910.
(45) Anastasiadis, S. H.; Chrissopoulou, K.; Frick, B. Structure and Dynamics in Polymer/Layered Silicate Nanocomposites. *Mater. Sci. Eng., B* **2008**, *152*, 33−39.
(46) Vo, L. T.; Anastasiadis, S. H.; Giannelis, E. P. Dielectric Study of Poly(styrene-co-butadiene) Composites with Carbon Black, Silica and Nanoclay. *Macromolecules* **2011**, *46*, 6162−6171.
(47) Barroso-Bujans, F.; Fernandez-Alfonso, F.; Cerveny, S.; Parker, S. F.; Alegria, A.; Colmenero, J. Polymers under Extreme Two-dimensional Confinement: Poly(ethylene oxide) in Graphite Oxide. *Soft Matter* **2011**, *16*, 7173−7176.
(48) Barroso-Bujans, F.; Cerveny, S.; Alegria, A.; Colmenero, J. Chain Length Effects on the Dynamics of Poly(ethylene oxide) Confined in Graphite Oxide: A Broadband Dielectric Spectroscopy Study. *Macromolecules* **2013**, *46*, 7932−7939.
(49) Alexandris, S.; Sakellariou, G.; Steinhart, M.; Floudas, G. Dynamics of Unentangled cis-1,4-Polyisoprene Confined to Nanoporous Alumina. *Macromolecules* **2014**, *47*, 3895−3900.
(50) Pinnavaia, T. J.; Beall, G. W. *Polymer-Clay Nanocomposites*; John Wiley & Sons: West Sussex, U.K., (2000).
(51) Sinha Ray, S.; Okamoto, M. Polymer/Layered Silicate Nanocomposites: A Review from Preparation to Processing. *Prog. Polym. Sci.* **2003**, *28*, 1539−1641.
(52) Tjong, S. C. Structural and Mechanical Properties of Polymer Nanocomposites. *Mater. Sci. Eng., R* **2006**, *53*, 73−197.
(53) Chrissopoulou, K.; Altintzi, I.; Anastasiadis, S. H.; Giannelis, E. P.; Pitsikalis, M.; Hadjichristidis, N.; Theophilou, N. Controlling the Miscibility of Polyethylene/Layered Silicate Nanocomposites by Altering the Polymer/Surface Interactions. *Polymer* **2005**, *46*, 12440−12451.
(54) Chrissopoulou, K.; Altintzi, I.; Andrianaki, I.; Shemesh, R.; Retsos, H.; Giannelis, E. P.; Anastasiadis, S. H. Understanding and Controlling the Structure of Polypropylene/Layered Silicate Nanocomposites. *J. Polym. Sci., Part B: Polym. Phys.* **2008**, *46*, 2683−2695.
(55) Chrissopoulou, K.; Anastasiadis, S. H. Polyolefin/Layered Silicate Nanocomposites with Functional Compatibilizers. *Eur. Polym. J.* **2011**, *47*, 600−613.
(56) Fotiadou, S.; Chrissopoulou, K.; Frick, B.; Anastasiadis, S. H. Structure and Dynamics of Polymer Chains in Hydrophilic Nanocomposites. *J. Polym. Sci., Part B: Polym. Phys.* **2010**, *48*, 1658−1667.
(57) Lorthioir, C.; Laupretre, F.; Soulestin, J.; Lefebvre, J. M. Segmental Dynamics of poly(ethylene oxide) Chains in a Model Polymer/Clay Intercalated Phase: Solid State NMR Investigation. *Macromolecules* **2009**, *42*, 218−230.
(58) Prevosto, D.; Lucchesi, M.; Bertoldo, M.; Passaglia, E.; Ciardelli, F.; Rolla, P. Interfacial Effects on the Dynamics of Ethylene-propylene Copolymer Nanocomposite with Inorganic Clays. *J. Non-Cryst. Sol.* **2010**, *356*, 568−573.
(59) Labardi, M.; Prevosto, D.; Nguyen, K. H.; Capaccioli, S.; Lucchesi, M.; Rolla, P. Local Dielectric Spectroscopy of Nanocomposite Materials Interfaces. *J. Vac. Sci. Technol. B* **2010**, *28*, C4D11−17.
(60) Saiter, A.; Prevosto, D.; Passaglia, E.; Couderc, H.; Delbreilh, L.; Saiter, J. M. Cooperativity Length Scale in Nanocomposites: Interfacial and Confinement Effects. *Phys. Rev. E* **2013**, *88*, 042605.
(61) Decker, J. J.; Chvalun, S. N.; Nazarenko, S. Intercalation Behavior of Hydroxylated Dendritic Polyesters in Polymer Clay

DOI: 10.1021/am507571y
ACS Appl. Mater. Interfaces 2015, 7, 12387−12398

Nanocomposites Prepared from Aqueous Solutions. *Polymer* **2011**, *52*, 3943−3955.
(62) Hackett, E.; Manias, E.; Giannelis, E. P. Computer Simulation Studies of PEO/Layer Silicate Nanocomposites. *Chem. Mater.* **2000**, *12*, 2161−2167.
(63) Nguyen, H. K.; Labardi, M.; Lucchesi, M.; Rolla, P.; Prevosto, D. Plasticization in Ultrathin Polymer Films: The Role of Supporting Substrate and Annealing. *Macromolecules* **2013**, *46*, 555−561.
(64) Schoenhals, A.; Goering, H.; Schick, Ch.; Frick, B.; Zorn, R. Polymers in nanoconfinement: What can be Learned from Relaxation and Scattering Experiments? *J. Non-Cryst. Sol.* **2005**, *351*, 2668−2677.
(65) Schoenhals, A.; Goering, H.; Schick, Ch.; Frick, B.; Mayorova, M.; Zorn, R. Segmental Dynamics of Poly(methyl phenyl siloxane) Confined to Nanoporous Glasses. *Eur. Phys. J.: Spec. Top.* **2007**, *141*, 255−259.
(66) Bras, A. R.; Fonseca, I. M.; Dionisio, M.; Schonhals, A.; Affouard, F.; Correia, N. T. Influence of Nanoscale Confinement on the Molecular Mobility of Ibuprofen. *J. Phys. Chem. C* **2014**, *118*, 13857−13868.
(67) Serghei, A.; Mikhailova, Y.; Eichhorn, K.-J.; Voit, B.; Kremer, F. Discrepancies in the Characterizationof the Glass Transition in Thin Films of Hyperbranched Polyesters. *J. Polym. Sci., Part B: Polym. Phys.* **2006**, *44*, 3006−3010.
(68) Boucher, V. M.; Cangialosi, D.; Yin, H. J.; Schonhals, A.; Alegria, A.; Colmenero, J. T_g Depression and Invariant Segmental Dynamics in Polystyrene Thin Films. *Soft Matter* **2012**, *8*, 5119−5122.
(69) Zhang, C.; Boucher, V. M.; Cangialosi, D.; Pristley, R. D. Mobility and Glass Transition Temperature of Polymer Nanospheres. *Polymer* **2013**, *54*, 230−235.
(70) Ngai, K. L. Relaxation in Nanometer-size Polymers and Glass Formers: Application of the Coupling Model to some Current Problems. *Philos. Mag. B* **2002**, *82*, 291−303.

DOI: 10.1021/am507571y
ACS Appl. Mater. Interfaces 2015, 7, 12387−12398